# Study the Crystallization, Electroconductivity and Mechanical Properties in Selected Engineering Polymers and Blends

Ahmed Nasr, Ph.D.

Doctoral Thesis Summary

Tomas Bata University in Zlín

Tomas Bata University in Zlín

Doctoral Thesis Summary

# Study the Crystallization, Electroconductivity and Mechanical Properties in Selected Engineering Polymers and Blends

## Studium krystalizace, elektrické vodivosti a mechanických vlastností vybraných inženýrských polymerů a směsí


| | |
|---|---|
| Author: | Ahmed Nasr, Ph.D. |
| Degree programme: | P2808 Chemistry and Materials Technology |
| Degree course: | 2808v006 Technology of Macromolecular Compounds |
| Supervisor: | prof. Ing. Petr Svoboda, Ph.D. |
| External examiners: | prof. Ing. Pavel Mokrejš, Ph.D. |
| | Assoc. Ing. Antonín Kuta, Ph.D. |


Zlin, December 2023

Published by **Tomas Bata University in Zlín** in the Edition **Doctoral Thesis Summary.**
The publication was issued in the year 2023.

Key words in Czech: *Elektrická vodivost, krystalizace, tepelná degradace, optická mikroskopie, DSC, SAXS.*

Key words: *Electrical conductivity, Crystallization, Thermal degradation, Optical microscopy, DSC, SAXS.*

Full text of the doctoral thesis is available in the Library of TBU in Zlín.

ISBN 978-80-7678-216-7

# ABSTRACT

This doctoral thesis investigated the multifaceted interplay between crystallization dynamics, electroconductivity, and mechanical attributes within selected engineering polymers and their blends. The overarching objective was to unravel the intricate relationships governing these fundamental properties and their implications for advanced material applications.

Firstly, the influence of thermal degradation on the crystallization of Poly(butylene terephthalate) (PBT) was meticulously examined. The research revealed a substantial shift in the crystallization temperature, indicative of profound modification. This shift occurred through distinct phases, involving initial rise, steep decrease, and subsequent degradation-induced changes. The corresponding trends in crystallinity and crystallization kinetics were observed, with particular attention to the influence of differing lamellar thicknesses. These findings underscored the intricate nature of PBT's crystallization behavior under thermal degradation, contributing to a broader understanding of polymer degradation and its implications for crystallization processes.

Furthermore, the research delved into the intricate terrain of Poly(butylene terephthalate) crystallization kinetics, particularly in response to various fusion temperatures. The empirical results demonstrated a pivotal correlation between fusion temperature and the resultant heat flow curve, revealing a nuanced interplay between crystallinity and heat flow profile. The Ozawa and Avrami models were adeptly employed to elucidate crystallization kinetics, affirming the role of fusion temperature in nucleation and crystal growth mechanisms. These findings hold promise for optimizing processing parameters and enhancing material attributes across diverse applications.

Moreover, the intricate interplay between fusion temperature, duration, and nonisothermal crystallization kinetics in polyamide 6 (PA6) was explored. Employing advanced analytical techniques, the study unveiled insights into nucleation centers, crystallization temperature shifts, and kinetics. The models utilized effectively shed light on the complex relationship between fusion temperature and crystallization processes, furthering our comprehension of polymer material processing.

Lastly, the work explored the integration of carbon fibers within an elastic polymer matrix, yielding EOC/CF composites. The study meticulously analyzed the resulting mechanical attributes and morphology alongside implications for electroconductivity. The study demonstrated a marked enhancement in tensile modulus and stress through various analytical methodologies while maintaining elasticity. Moreover, the investigation delved into electrical properties, revealing a critical percolation threshold in the composites. These results suggest the potential for advanced composites, particularly for applications in electronics engineering.

This doctoral thesis comprehensively explores the intricate relationships among crystallization, electroconductivity, and mechanical attributes within engineering polymers and blends. The findings have far-reaching implications for material design and applications, paving the way for innovative advancements in diverse fields.

**Key words**: *Electrical conductivity, Crystallization, Thermal degradation, Optical microscopy, DSC, SAXS.*

# ABSTRAKT

Tato disertační práce se zabývala mnohostrannými interakcemi mezi dynamikou krystalizace, elektrickou vodivostí a mechanickými vlastnostmi vybraných technických polymerů a jejich kompozitů a směsí. Hlavním cílem bylo odhalit složité vztahy, jimiž se tyto základní vlastnosti řídí, a jejich důsledky pro aplikace pokročilých materiálů.

Nejprve byl pečlivě zkoumán vliv tepelné degradace na krystalizaci poly(butylentereftalátu) (PBT). Výzkum odhalil podstatný posun v teplotě krystalizace, což svědčí o hluboké modifikaci. K tomuto posunu došlo v různých fázích, které zahrnovaly počáteční nárůst, prudký pokles a následné změny vyvolané degradací. Byly sledovány odpovídající trendy v krystalinitě a kinetice krystalizace, přičemž zvláštní pozornost byla věnována vlivu na rozdílnou tloušťku lamel. Tato zjištění zdůraznila složitou povahu krystalizačního chování PBT při tepelné degradaci a přispěla k širšímu pochopení degradace polymerů a jejích důsledků pro krystalizační procesy.

Výzkum dále pronikl do složité oblasti kinetiky krystalizace poly(butylentereftalátu), zejména v závislosti na různých teplotách tavení. Empirické výsledky prokázaly klíčovou korelaci mezi teplotou tavení a výslednou křivkou tepelného toku a odhalily jemnou souhru mezi krystalinitou a profilem tepelného toku. K objasnění kinetiky krystalizace byly vhodně použity Ozawův a Avramiho model, které potvrdily roli teploty tavení v mechanismech nukleace a růstu krystalů. Tato zjištění jsou příslibem pro optimalizaci parametrů zpracování a zlepšení vlastností materiálu v různých aplikacích.

Kromě toho byla zkoumána složitá souhra mezi teplotou tavení, dobou trvání a kinetikou neizotermické krystalizace v polyamidu 6 (PA6). S využitím pokročilých analytických technik studie odhalila poznatky o nukleačních centrech, teplotních posunech a kinetice krystalizace. Použité modely účinně osvětlují složitý vztah mezi teplotou tavení a krystalizačními procesy a prohlubují naše porozumění zpracování polymerních materiálů.

Nakonec práce zkoumala integraci uhlíkových vláken do elastické polymerní matrice, čímž vznikly kompozity EOC/CF. Studie pečlivě analyzovala výsledné mechanické vlastnosti a morfologii spolu s důsledky pro elektrickou vodivost. Studie prokázala výrazné zvýšení modulu pružnosti v tahu a napětí pomocí

různých analytických metodik při zachování elasticity. Kromě toho se zkoumaly elektrické vlastnosti a odhalil se kritický práh perkolace v kompozitech. Tyto výsledky naznačují potenciál pokročilých kompozitů, zejména pro aplikace v elektronice.

Tato disertační práce komplexně zkoumá složité vztahy mezi krystalizací, elektrickou vodivostí a mechanickými vlastnostmi v rámci technických polymerů a směsí. Zjištění mají dalekosáhlé důsledky pro konstrukci a aplikace materiálů a otevírají cestu k inovativnímu pokroku v různých oblastech.

**Klíčová slova:** *Elektrická vodivost, krystalizace, tepelná degradace, optická mikroskopie, DSC, SAXS.*

# CONTENTS

# LIST OF PAPERS

1. **Influence of Thermal Degradation on the Crystallization of Poly(butylene terephthalate)**

   Ahmed Nasr * and Petr Svoboda

   Accepted in Express Polymer Letters Journal, December 2023.

2. **Effect of fusion temperature on the crystallization kinetics of poly(butylene terephthalate)**

   Ahmed Nasr * and Petr Svoboda

   Published in journal of CrystEngComm, 2023. 25(34):4848-4855.
   DOI: 10.1039/D3CE00669G

3. **Influence of Fusion Temperature on Nonisothermal Crystallization Kinetics of Polyamide 6**

   Ahmed Nasr * and Petr Svoboda

   Published in journal of Polymers, 2023;15(8):1952.

   DOI: 10.3390/polym15081952

4. **Elastic Electrically Conductive Composites Based on Vapor-Grown Carbon Fibers for Use in Sensors**

   Ahmed Nasr *, Ondřej Mrhálek and Petr Svoboda

   Published in journal of Polymers, 2023;15(9):2005.

   DOI: 10.3390/polym15092005

# AIM OF WORK

The primary objective of this research is to comprehensively investigate and analyze the intricate interplay between crystallization kinetics, electric conductivity, and mechanical properties within selected engineering polymers and their composites and blends. This work aims to unravel the underlying mechanisms governing these fundamental properties and their interdependencies, providing valuable insights into the design, optimization, and application of advanced materials with enhanced functionalities.

By studying the influence of factors such as fusion temperature, thermal degradation, and filler incorporation on crystallization behaviour, this research seeks to uncover the underlying principles that govern the crystalline structure and kinetics of polymers. Furthermore, by assessing the electric conductivity of polymer composites, a deeper understanding of their electrical behaviour will be achieved, allowing for potential applications in fields like electronics engineering and sensor technology.

Another pivotal objective of this work is to analyze the mechanical properties of engineered polymers and their composites. Investigating the tensile modulus, stress-strain behaviour, and viscoelastic properties contributes to comprehending how these materials respond to mechanical stresses and strains. This knowledge can lead to developing materials with tailored mechanical properties suitable for various industrial and engineering applications.

Overall, this thesis aims to bridge the gaps between these interconnected properties and establish a comprehensive understanding of how they influence each other. This understanding, in turn, can inform the design and fabrication of innovative materials with improved properties, enabling advancements in fields ranging from materials science and polymer engineering to electronics and beyond.

# 1. THEORITICAL BACKGROUND

## 1.1. Introduction

Polymers exhibit diverse properties, including their crystallization ability, influenced by temperature and molecular weight distribution, impacting their mechanical strength [1, 2]. In terms of elasticity, polymers can display both elastomeric and rigid characteristics, making them versatile for various applications. Additionally, the electrical conductivity of polymers can be modified by incorporating conductive fillers, enabling their use in electrically conductive materials when factors like filler content and morphology are carefully controlled [3].

In polymer science and engineering, crystallization is crucial in determining polymers' physical and mechanical properties. The crystallization process involves transforming a disordered polymer melt into a crystalline structure, influenced by various factors such as thermal degradation, fusion temperature, fusion time, and polymer morphology [4]. Polymer crystallization is a complex process that involves multiple stages, including nucleation, growth, and final morphology development. Several factors, such as degradation, temperature, cooling rate, and molecular weight, influence these stages' kinetics. Fusion temperature, the temperature at which a polymer is melted, significantly impacts the crystallization process [5].

In general, reduced fusion temperatures result in an accelerated crystallization rate, increased crystalline structure, and diminished crystal dimensions. Specific engineering polymers, such as polyamide 6 (PA6) and Polybutylene Terephthalate (PBT), possess distinct characteristics that render them apt for various industrial uses. The influence of fusion temperature, thermal degradation, fusion time, and morphology on the crystallization process of these polymers has been extensively studied [6, 7]. Differential scanning calorimetry (DSC) and polarized optical microscopy (O.M.) are commonly used techniques to analyze the crystallization kinetics of these polymers.

Incorporating conductive fillers, such as carbon fibres, in polymer matrices can lead to materials with elastic and electrically conductive properties. The electrical conductivity of polymer blends depends on factors such as filler content, morphology, and the nature of the polymer matrix [8]. The percolation threshold, the minimum filler content required to achieve electrical conductivity, is an essential parameter in designing electrically conductive polymers [9]. Investigating the electrically conductive properties of EOC/CF blends can provide

valuable insights into their potential applications in electronics, sensors, and actuators.

This thesis focuses on selected engineering polymers and blends, specifically PA6, PBT, EOC and EOC/PBT blends. The study will provide valuable insights into the crystallization kinetics, elastic electrically conductive properties, and morphology of these materials, thus contributing to optimizing their design for specific applications. The findings of this research will benefit various industries, including automotive, aerospace, electronics, and construction, seeking to develop high-performance materials with tailored properties.

## 1.2. Crystallization Kinetics

Polymers are widely used materials with a broad range of applications due to their unique properties. One of the key properties of polymers is their ability to crystallize. Crystallization is the process of polymers forming an ordered, solid structure from a disordered liquid state. The kinetics of crystallization are essential to consider when processing polymer materials. There are two main types of crystallization kinetics: isothermal and nonisothermal crystallization [10].

### 1.2.1 Isothermal crystallization

Isothermal crystallization refers to the process by which a polymer is carried outat a constant temperature and allowed to crystallize. The kinetics of isothermal crystallization can be described using several models, including the Avrami and Ozawa models [11].

The Avrami model assumes that the crystallization rate is proportional to the amount of uncrystallized material remaining. This model assumes that the nucleation and growth of crystalline structures occur simultaneously and uniformly throughout the polymer melt [12].

The Ozawa model is dependent on the Avrami model, but it accounts for the effect of the degree of undercooling on the crystallization rate. The degree of undercooling refers to the difference between the crystallization temperature and the polymer's melting temperature. The Ozawa model can also be applied to the nonisothermal crystallization kinetics of polymers.

### 1.2.2 Nonisothermal crystallization

Nonisothermal crystallization refers to the process by which a polymer is heated or cooled at a specific rate and allowed to crystallize. Nonisothermal crystallization kinetics can be described using several models, including the Kissinger and Hoffman-Lauritzen models.

The Ziabicki model assumes that the rate of crystallization is corresponding to the degree of undercooling and the number of active nuclei. The degree of undercooling is the difference between the crystallization temperature and the equilibrium melting temperature of the polymer, and the number of active nuclei is a measure of the degree of crystallization. The Ziabicki model also accounts for the effect of crystal growth on the crystallization rate. This model has been used to describe the nonisothermal crystallization of several polymer materials, including polyethylene, polypropylene, and polycarbonate.

On the other hand, the Nakamura model assumes that the crystallization rate is proportional to the degree of undercooling and the nucleation rate. The rate of nucleation is a measure of the number of nucleation sites in the polymer melt. The Nakamura model also accounts for the effect of crystal growth on the rate of crystallization. This model has been used to describe the nonisothermal crystallization of several polymer materials, including polyethylene, polypropylene, and polyamide.

## 1.3. Electric Conductivity in Polymers

Introducing conductive additives, like carbon fibres, into polymer matrices can yield flexible and electrical conductivity materials. The electrical conductance of polymer combinations is influenced by elements such as the quantity of additives, the material's structure, and the inherent properties of the polymer matrix. The percolation threshold, which denotes the minimum amount of additives needed for electrical conductivity, is a critical parameter when formulating electrically conductive polymer mixtures. An exploration into the electrical conductive characteristics of EOC/CF blends has the potential to offer valuable insights into their prospective applications in fields like electronics, sensors, and actuators.

## 1.4. Morphology and its Influence on Properties

The morphology of polymers and blends is critical in determining their mechanical, thermal, and electrical properties. Factors such as crystallinity, phase separation, and interface adhesion can influence the performance of the materials. In the case of PA6, PBT, PHB, and EOC/CF blends, the morphology is closely

related to the crystallization kinetics and elastic electrically conductive properties. Studying the relationship between these materials' morphology, crystallization kinetics, and electrical conductivity can contribute to their efficient design and application.

## 1.5. Polymer Materials:

### 1.5.1. Polyamide 6 (PA6)

Polyamide 6 (PA6) is a semi-crystalline thermoplastic material renowned for its remarkable combination of high strength, toughness, and stiffness, rendering it a highly appealing choice for many applications [1, 2]. During processing PA6, the fusion temperature plays a pivotal role in governing the polymer's crystallization characteristics [3, 4]. The crystallization patterns of polyamide 6 are subject to the influence of several variables, including temperature, cooling rate, and molecular weight [5]. Notably, most polyamides, called nylons, exhibit a linear structure characterized by recurring amide units. These amide groups facilitate hydrogen bonding within the polymer chain, a phenomenon of paramount importance in shaping the material's physical and chemical attributes [2, 6]. Establishing hydrogen bonds within PA6 yields a robust, inflexible, and crystalline framework, contributing significantly to the material's elevated levels of strength, stiffness, and thermal resilience. Furthermore, this distinctive configuration of chemical bonds confers impressive resistance to chemical agents and low moisture absorption to polyamides, rendering them exceptionally well-suited for various textiles, automotive manufacturing, and electronics applications.

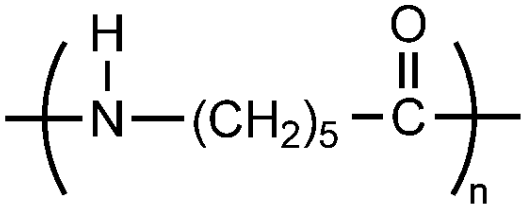


*Figure 1. PA6 formula.*

### 1.5.2. Polybutylene terephthalate (PBT)

Polybutylene terephthalate (PBT) is a world-wide semi-crystalline thermoplastic. It belongs to the group of polyesters together with, for example, polyethylene and polycarbonate, so it contains at least one ester bond. PBT typically has a crystallinity of around 35-40%. The glass transition temperature is in the range of 30-50°C and the melting point is usually between 222-232°C. It is fiber-forming, chemically resistant, has high strength and rigidity and low moisture content [13, 14].

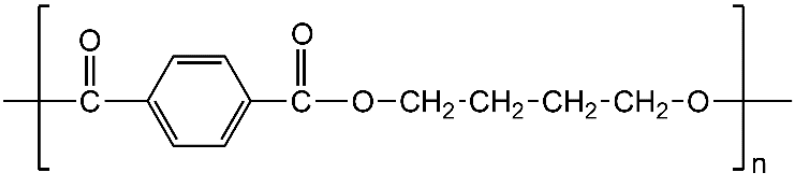

*Figure 2. The chemical formula of PBT.*

### 1.5.3. Ethylene-octane copolymer (EOC)

Another polymer used was ethylene-octane copolymer. In our case, a polymer called EOC39 was used, where the number 39 represents the mass percentage of the octane monomer. EOC39 has good flow characteristics, a melt flow index of 0,50 g/10 min (at 190 °C and load 2,16 kg) and a density of 0,868 g/cm3. The polymer is resistant to peroxides silanes. It has a melting point of 55 °C and a glass transition temperature of -52 °C. The properties of EOC39 are enhanced in mixtures with polypropylene and polyethylene [15-17].

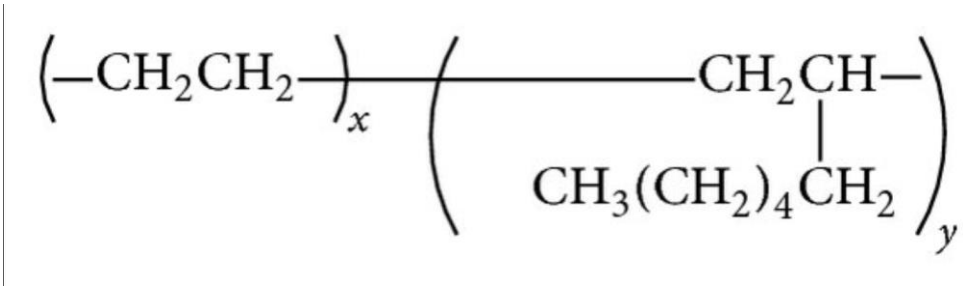

*Figure 3. The structural formula of Ethylene-octene copolymer [18].*

### 1.5.4. EOC/PBT Blend

PBT/EOC mixtures were prepared using the Haake Minilab extruder under the following conditions: 250 °C, 50 rpm and 9 minutes. An overview of all prepared mixtures and pure PBT is given in the table 1 and Figure 4 below.

Table 1: Overview of prepared mixtures

| Mixture | hm.% PBT | hm.% EOC |
|---|---|---|
| EOC/PBT | 30 | 70 |
| EOC/PBT | 32. 5 | 67. 5 |
| EOC/PBT | 35 | 65 |
| EOC/PBT | 37. 5 | 62. 5 |
| EOC/PBT | 40 | 60 |
| PBT | 100 | - |

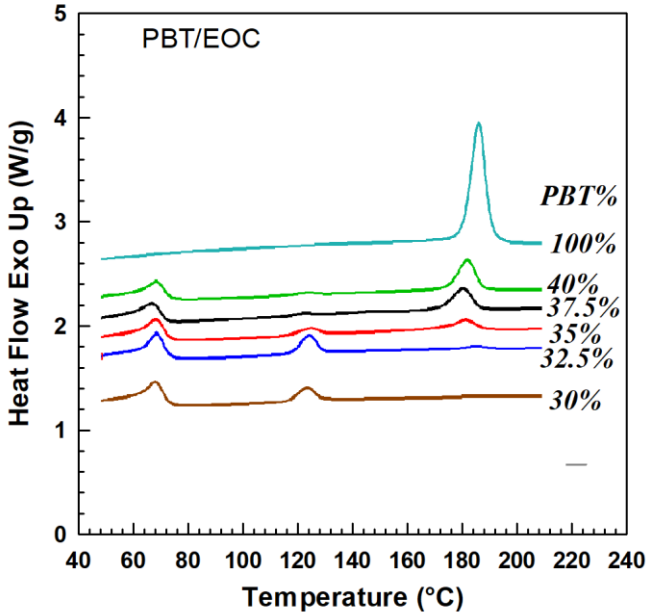


*Figure 4. DSC curves of PBT/EOC blend and pure PBT.*

## 1.6. Experimental Methods

### 1.6.1. Differential Scanning Calorimetry (DSC)

Differential scanning calorimetry (DSC) measurements were performed on the polymer samples to study their crystallization kinetics and thermal properties. The samples were heated and cooled at different rates, and the resulting DSC curves were analyzed to obtain crystallization and melting temperatures [19, 20].

The measurement is carried out in an inert atmosphere and two pans, one empty, the reference and the other containing the sample to be examined. Each pan has its heating device, which must change the temperature at the same rate [21].

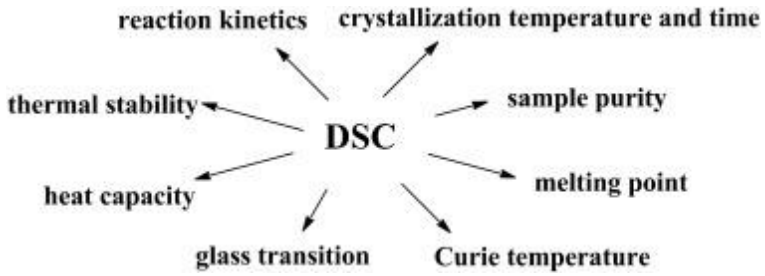


*Figure 5. Applications of DSC [20].*

### 1.6.2. Electrical Conductivity Measurements

A strain gauge is employed to assess the sample's electrical resistance. This strain gauge is a sensor with an electrical resistance that varies in response to applied force. The calibration procedure entails utilizing different weights. During calibration, the sensor's zero offset and linearity are scrutinized by comparing its output when subjected to reference weights. Adjustments to the sensor are made as necessary [22]. The measurement of electrical resistance is executed using a multimeter configured in ohms, and the obtained values are subsequently compared with the manufacturer's calibration certificate to ascertain their close correspondence.. The dependence of the electrical conductivity on the carbon fibre content and blend morphology was investigated to understand the percolation behaviour and the role of filler dispersion and distribution [23, 24].

### 1.6.3. Scanning Electron Microscopy (SEM)

Scanning electron microscopy (SEM) was employed to examine the morphology of the selected polymers and blends. The samples were cryogenically fractured, sputter-coated with a thin layer of conductive material, and then observed under high vacuum conditions to obtain high-resolution images of the fracture surfaces [25-27].

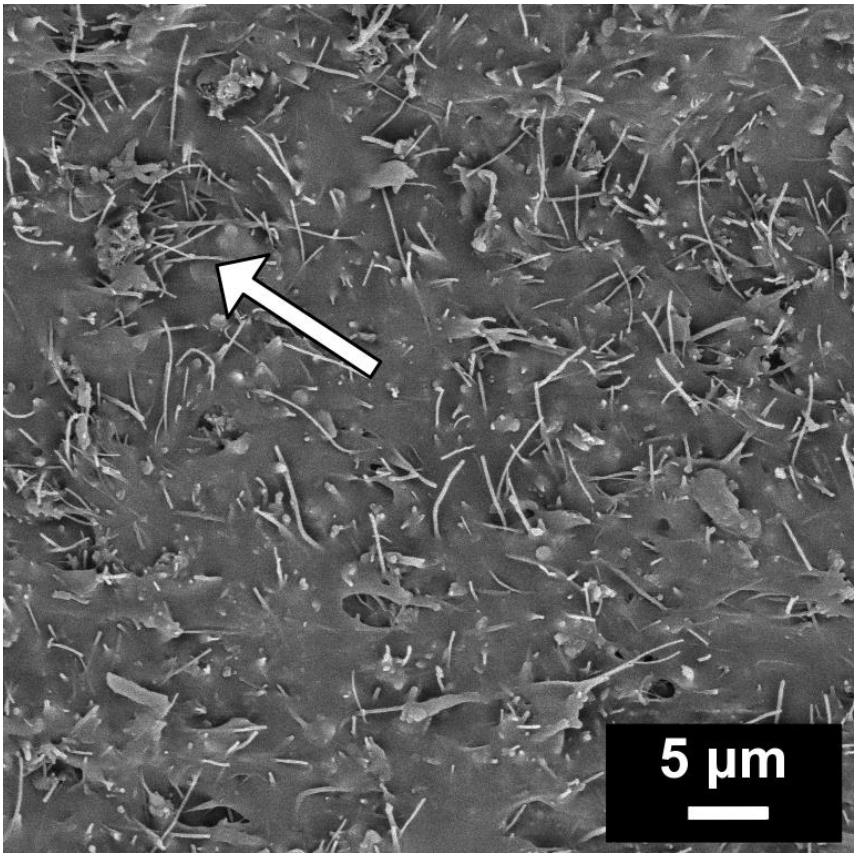


*Figure 6. SEM image of EOC/CF composite with 30 wt.% of C.F. [25].*

### 1.6.4. Small Angle X-ray Scattering (SAXS)

Small-angle X-ray scattering (SAXS) is a non-destructive analytical technique employed to probe nanostructures present in both liquid and solid substances. In a SAXS experiment, a focused X-ray beam is directed at a nanostructured specimen, encompassing substances like proteins, macromolecules, or nanoparticle dispersions. The scattering pattern generated during this process varies depending on the size of the particles within the sample, yielding valuable insights into their dimensions and size distribution. What sets SAXS apart is its ability to offer representative structural information covering a substantial sample area. This feature distinguishes it from microscopic methods, which may provide detailed data but are often limited in their capacity to capture the overall structural characteristics of a sample. Consequently, SAXS is an excellent complementary method, particularly when assessing the specific surface area of materials, enhancing our understanding of nanoscale structures and their properties in diverse scientific applications. [28, 29].

### 1.6.5. Twin Screw Extruder

A twin screw extruder, often called a twin-screw extruder, is a machinery utilized within the plastics sector to manipulate and blend plastic substances. This device comprises a closed barrel housing two screws interning and rotating on splined shafts. The screws are precisely meshed and turn unison, facilitating thorough material mixing and shaping. Twin-screw extruders have extensive application in processing powder blends, requiring meticulous blending and reactive extrusion processes [30-32].

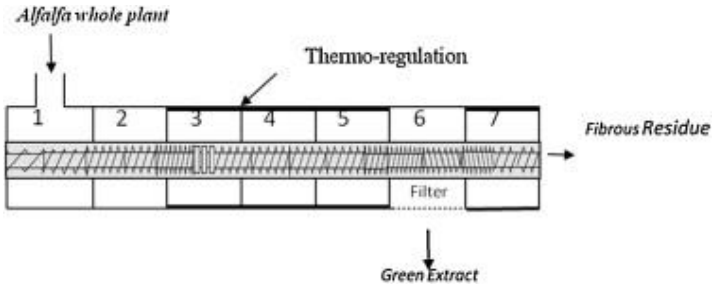


*Figure 7. Schematic representation of the twin-screw extruder barrel [33].*

### 1.6.6. Mechanical Testing

Mechanical properties of the selected polymers and blends, such as tensile strength, elongation at break, and modulus, were determined using a universal testing machine. The specimens were prepared according to the relevant standards, and the tests were conducted at a constant strain rate [34-36].

# 2. RESULTS

In this section, the results of the influence of the fusion temperature and thermal degradation on the crystallization kinetics of PA6 and PBT will be shown. Additionally, we will also show the results of our work that concern the electrical and mechanical properties of EOC/CF composites.

## 2.1. Crystallization Kinetics Results

The fusion temperature has a significant effect on the crystallization kinetics of Polyamide6 (PA6). Figure 8 illustrates the impact of different fusion temperatures on the heat flow [37], in which PA6 samples were heated at various fusion temperatures from 225 °C to 245 °C for 2 min and then were cooled at a cooling rate of 25 °C/min. The graph demonstrates that with increasing fusion temperature, the exothermic trace becomes narrower and shifts toward lower temperatures, then it becomes wider but still moves toward lower temperatures. At lower fusion temperatures, some crystals remain unmelted, which act as nucleation centers. As the fusion temperature increases, more crystals melt, leading to smaller nucleation centres. Consequently, crystallization becomes more challenging, requiring a higher degree of supercooling. Therefore, the crystallization temperature shifts towards lower temperatures. This change is most noticeable in the temperature range of 225–242 °C, and then the peak remains at approximately the same temperature as the fusion temperature increases.

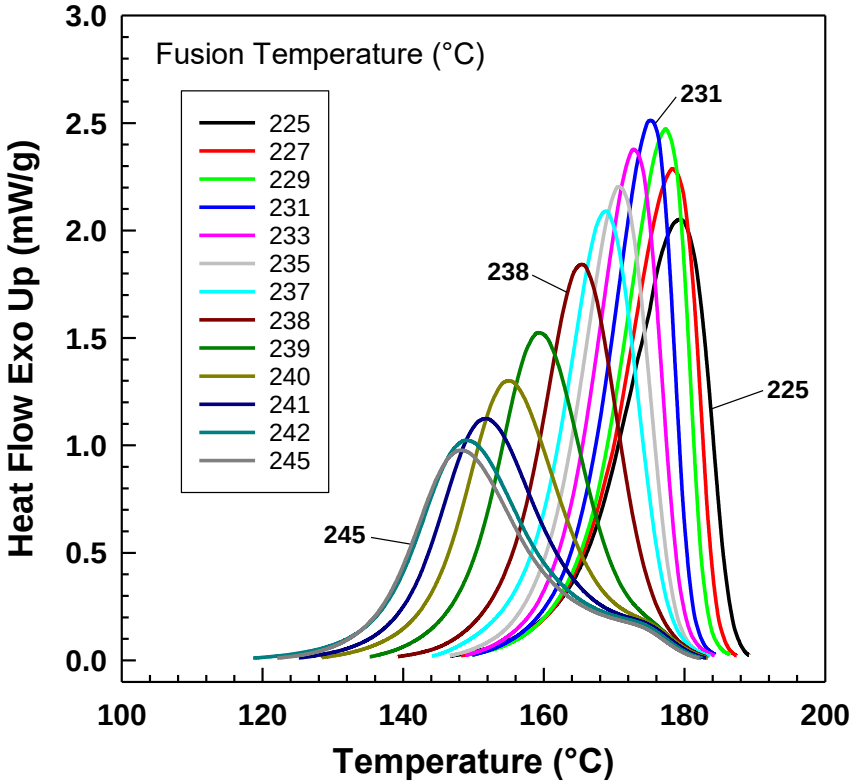


*Figure 8. Exothermic heat flow of PA6 from DSC after various fusion temperatures at a cooling rate of 25 °C/min.*

The presence of shoulder on some of the heat flow curves suggests the presence of "transcrystallinity" described by Freire et al. [38], meaning differences in crystallization kinetics on the surface (in contact with aluminum pan) and inside the pellet. Thickness of the sample seems to be very important. For our polarized optical microscopy measurement, it was necessary to use thicker sample (more than 100 μm) in order to be able to observe spherulites.

However, in terms of crystallization kinetics, the inverse value of crystallization is preferable. Conversely, this value decreases with increasing fusion temperature, indicating that crystallization kinetics are slowing.

Polarized optical microscopy (O.M.) is used to observe the morphology of PA6 spherulites formed during nonisothermal crystallization. These spherulites are spherical and exhibit highly ordered Maltese cross-pattern structures [39, 40]. Understanding the details of the spherulite morphology and growth rate is crucial for controlling the final product's physical properties. Figure 9 presents O.M. images of PA6 that have undergone a cooling process from 200 °C to 100 °C at a rate of 20 °C/min. During this cooling process, the sample begins to crystallize. The results indicate that spherulites are present during the cooling process. These spherulites have a circular cross-section and exhibit a Maltese cross-pattern system, which suggests that they are oriented along or perpendicular to the crystalline molecular axis concerning the spherulitic radius [41].

The size of the crystallites is highly dependent on the crystallization temperature and time. Figure 10 illustrates the impact of temperature on the rate of spherulite formation during the crystallization process. These spherulite structures are formed due to many nucleation sites and the rapid cooling of the molten polymer, which impedes normal crystal growth.

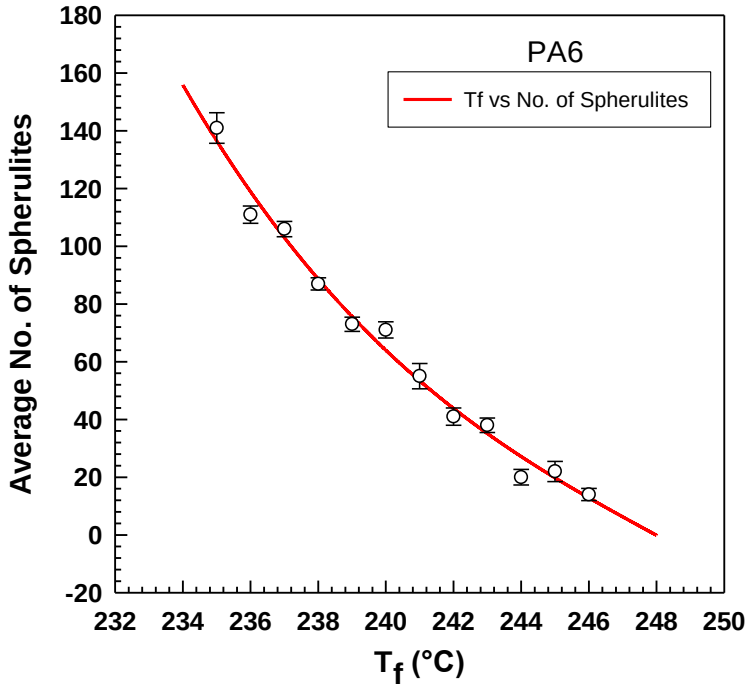


***Figure 9.*** *Effect of the fusion temperature on the number of spherulites of PA6 crystallization.*

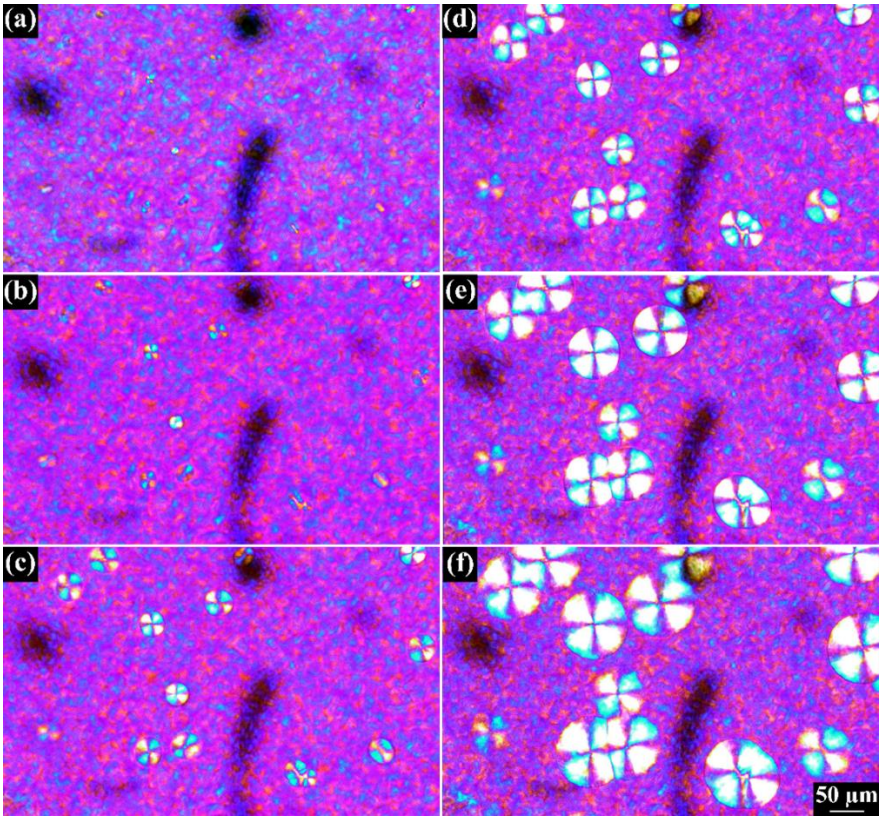


***Figure 10. PA6*** *Nonisothermal crystallization by polarized optical microscope at 20 °C/min cooling rate at different temperatures (**a**) 186.3 °C, (**b**) 183 °C, (**c**) 179.6 °C, (**d**) 176.3 °C, (**e**) 173.8 °C, (**f**) 169.8 °C.*

Figure 11 shows the melting temperature analysis as a function of crystallization temperature that was performed according to the Hoffman–Weeks theory. Where the extrapolated line crosses the Tm = Tc line, one can find an equilibrium melting point $T_m^0$. Our $T_m^0$ was found to be at 242 °C, which is very close to Wang et al. who reported the equilibrium melting point for pure PA6 to be about 243 °C [42].

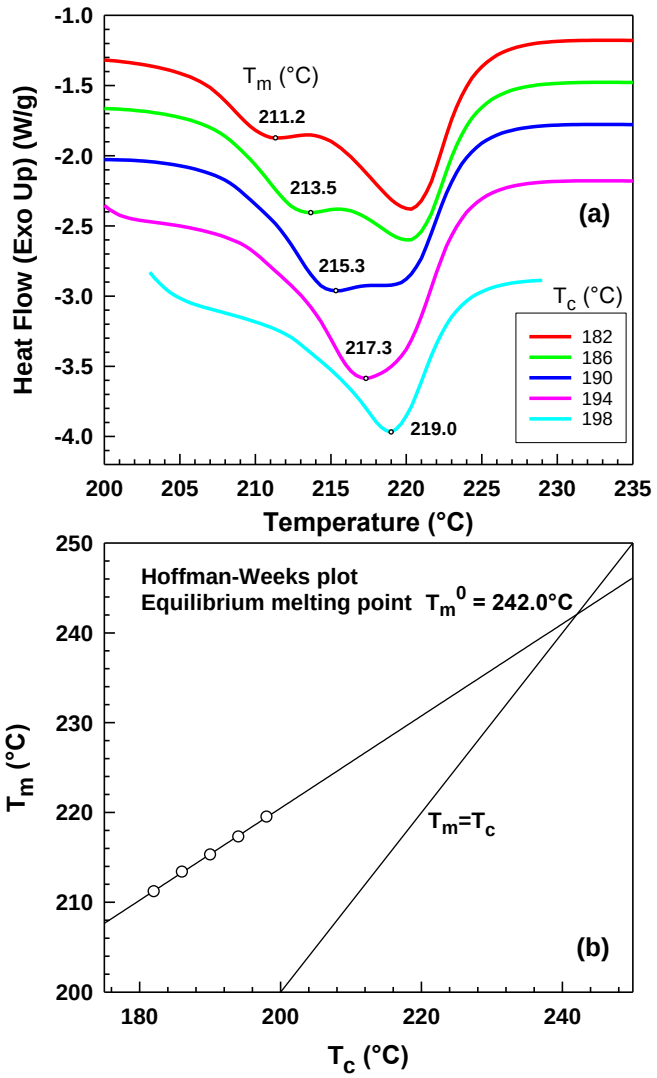


***Figure 11.*** *(**a**) Determination of melting temperature after isothermal crystallization of PA6 at various temperatures, (**b**) Hoffman–Weeks plot for equilibrium melting point determination, melting point of peak I vs. crystallization temperature.*

For PBT S-curve, which illustrates relative crystallinity, can demonstrate the effect of applying various fusion temperatures on the crystallization kinetics [43]. Figure 12 presents the relative crystallinity curves of PBT corresponding to different fusion temperatures (232–244°C). A notable trend is observed; with an increase in fusion temperature, there is a subsequent decrease in crystallinity, as shown in Table 2. Furthermore, this decrease is accompanied by shifting the S-curve towards lower temperatures. This phenomenon can be elucidated by referring to the thermodynamics involved in the crystallization process. At elevated temperatures, an enhancement in molecular mobility and crystal growth

is generally observed, extending the duration required to achieve a specific degree of crystallinity [44, 45].

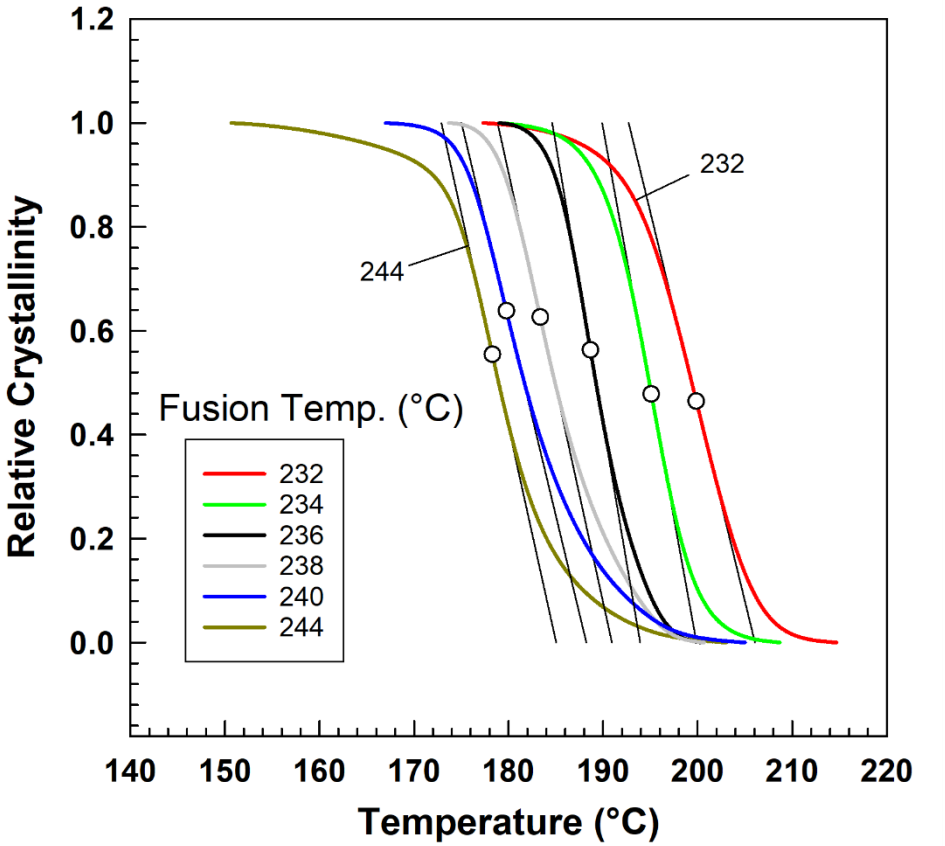


*Figure 12. Relative crystallinity vs. temperature.*

Many researchers use the Avrami plot to evaluate isothermal crystallization (see Figure 13) [46-48]. One can evaluate the Avrami constants n and k from this plot. These two constants are listed in Table 2. Interconnected two parameters describe the S-curve, and the trend of rate constant k is unclear. Therefore, we have used Nakamura's rate constant $K = k^{1/n}$ that shows a better trend (even though it was originally developed for nonisothermal crystallization).

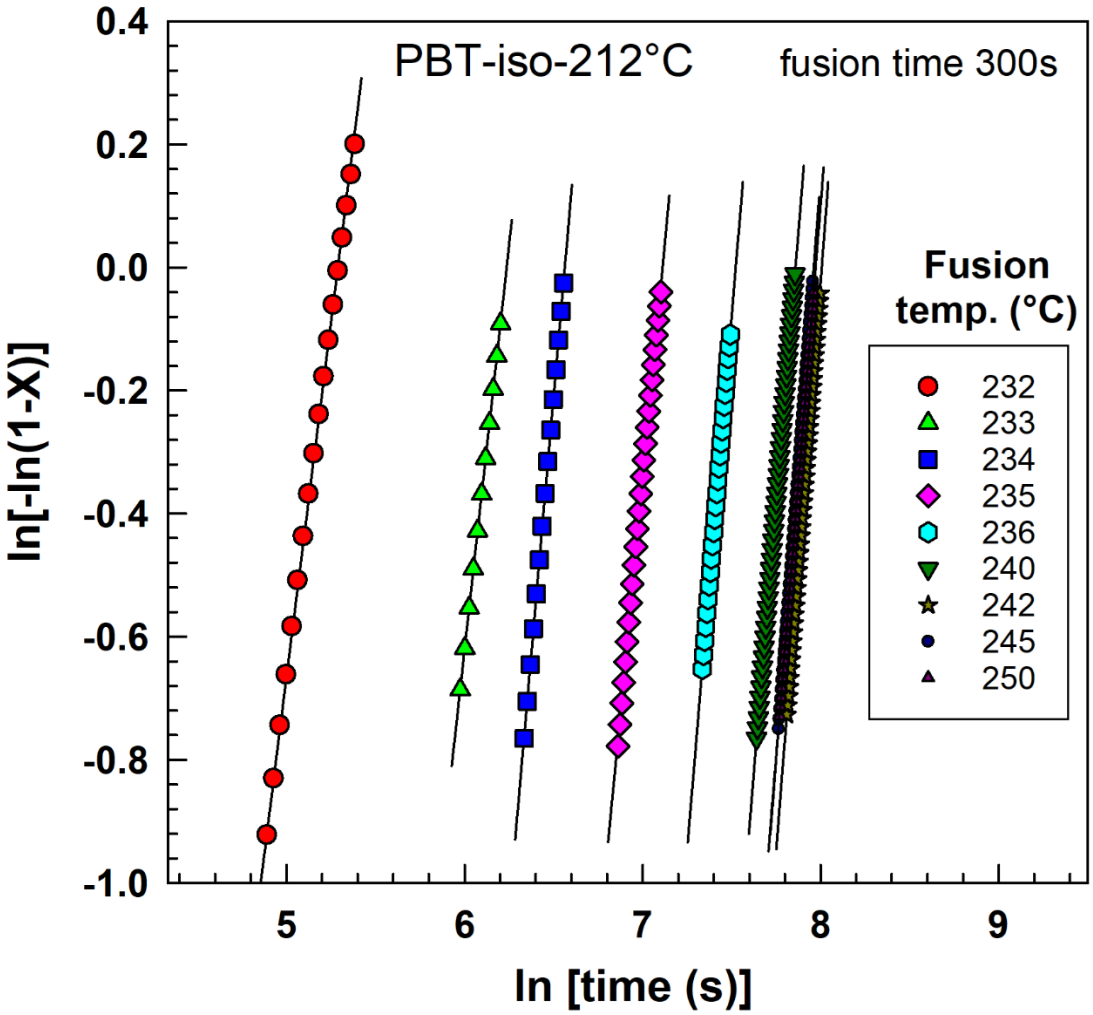


*Figure 13. Avrami plot from isothermal crystallization at 212°C after melting at various fusion temperatures by DSC.*

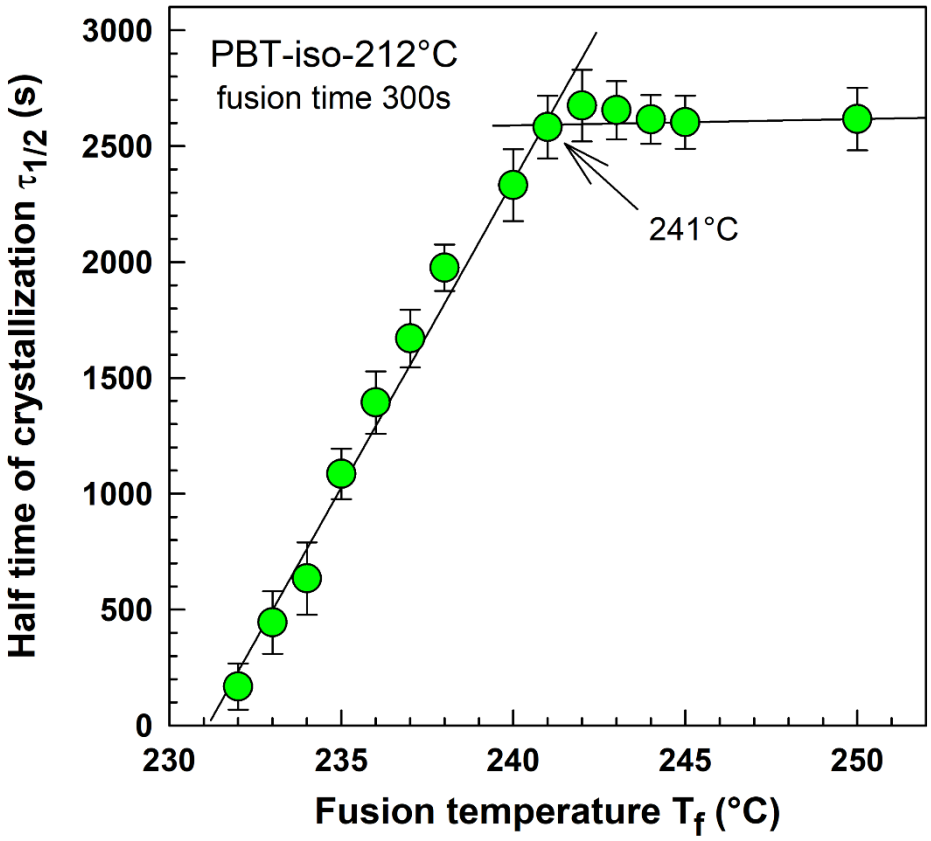


*Figure 14. PBT Half-time of crystallization $\tau_{1/2}$ as a function of fusion temperature $T_f$, from isothermal crystallization at 212°C.*

In our work, we used the slope at the inflection point of the S-curve to evaluate crystallization kinetics. The slopes are listed in Table 2 and show a clear decreasing trend in the range 232-242°C, and then the kinetics stabilizes in the range 242-250°C fusion temperature range.

**Table 2.** PBT Isothermal crystallization kinetics parameters at **212°C** from DSC.

| **Fusion temp.** | **Crystallization Half time** | **One over half time of crystallization** | **Slope at inflection** | **Avrami** | | **Nakamura** |
|---|---|---|---|---|---|---|
| $T_f$ (°C) | $\tau_{1/2}$ (s) | $\tau_{1/2}^{-1}$ (s-1) | s-1 | $n$ | $k$ | $K = k^{1/n}$ |
| 232 | 168 | 0.0059482 | 0.0050558 | 2.310 | 4.956E-06 | 0.0050482 |
| 233 | 444 | 0.0022508 | 0.0020843 | 2.629 | 7.582E-08 | 0.0019570 |
| 234 | 634 | 0.0015769 | 0.0015346 | 3.339 | 3.044E-10 | 0.0014119 |
| 235 | 1085 | 0.0009213 | 0.0010449 | 3.058 | 3.593E-10 | 0.0008155 |
| 236 | 1394 | 0.0007174 | 0.0007253 | 3.470 | 4.617E-12 | 0.0005408 |
| 240 | 2332 | 0.0004288 | 0.0005223 | 3.510 | 1.045E-12 | 0.0003862 |
| 241 | 2582 | 0.0003873 | 0.0004958 | 3.682 | 2.689E-13 | 0.0003855 |
| 242 | 2675 | 0.0003738 | 0.0004739 | 3.712 | 1.235E-13 | 0.0003334 |
| 243 | 2655 | 0.0003766 | 0.0004889 | 3.568 | 5.569E-13 | 0.0003677 |
| 244 | 2616 | 0.0003823 | 0.0004985 | 3.689 | 1.569E-13 | 0.0003381 |
| 245 | 2603 | 0.0003841 | 0.0005014 | 3.772 | 9.080E-14 | 0.0003485 |
| 250 | 2617 | 0.0003821 | 0.0004757 | 3.593 | 3.636E-13 | 0.0003450 |

Thermal degradation has a great effect on the crystallization kinetics of PBT. Several authors have reported a change in melting point $T_m$ towards lower values during degradation [49-52]. Figure 15 shows the change in melting temperature by the thermal degradation at 270°C. Increasing the degradation time, the peak shifts to lower temperatures and then two melting points appear ($T_{m1}$ and $T_{m2}$).

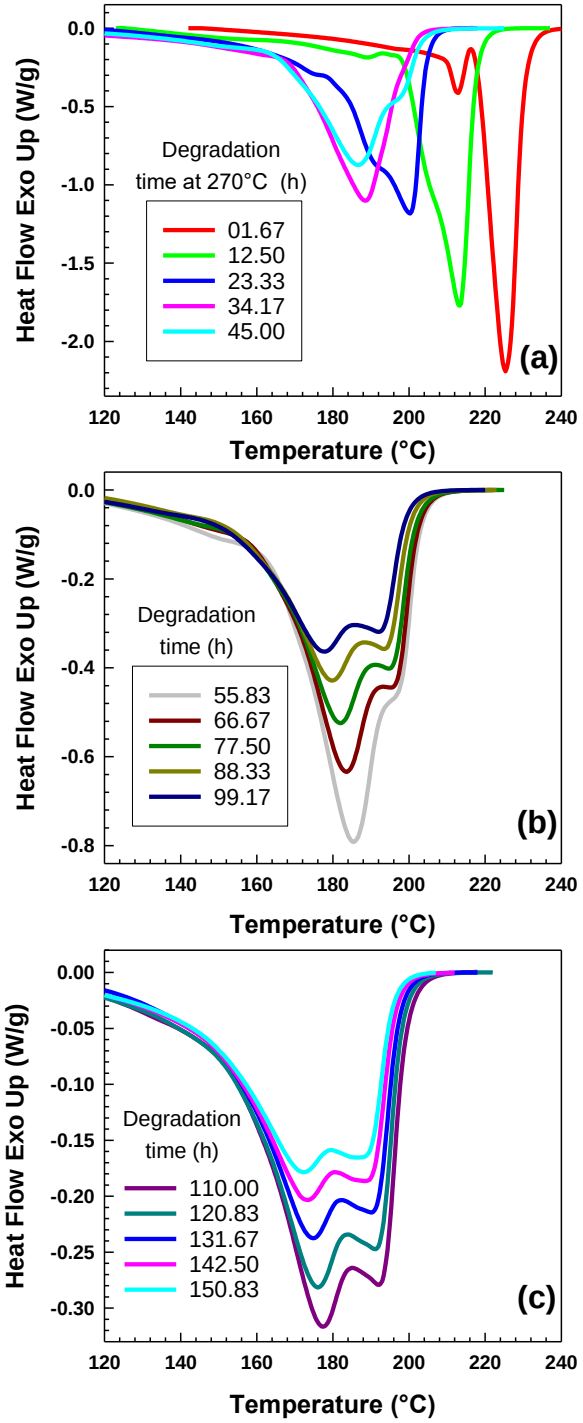


*Figure 15. Change in melting behaviour by the thermal degradation at 270°C.*

We have observed a decrease in melting point during the degradation. Based on the Gibbs-Thomson equation, we can assume that the lamellar thickness decreases during degradation. Initially, there is mainly one peak (even though the second peak is also present). The situation during the initial part of degradation could be graphically represented by Figure 17. In the later part of degradation, the presence of two peaks is evident and suggests the presence of lamellae with two different thicknesses (see Figure 18).

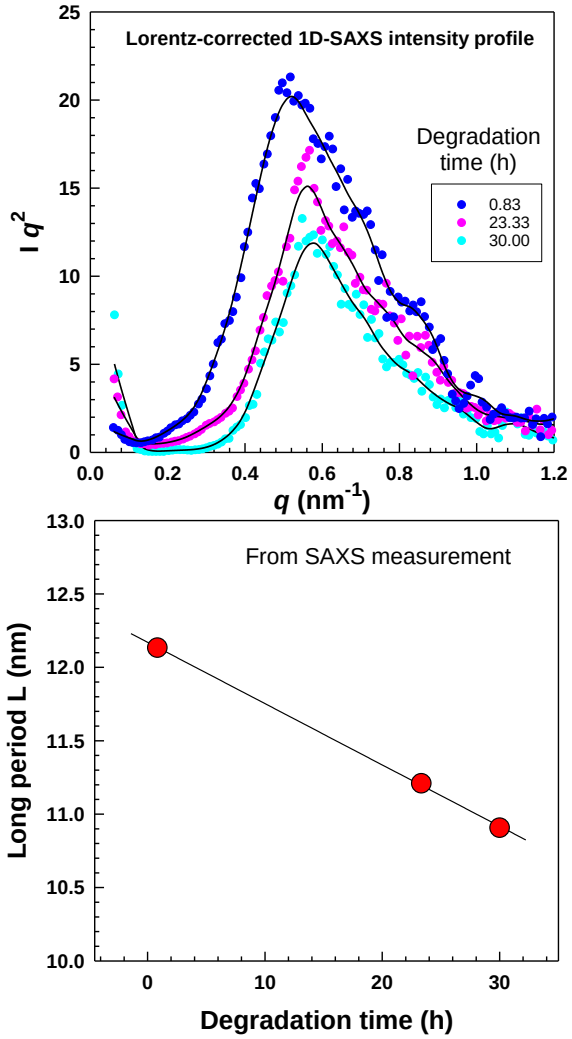


*Figure 16. (a) Lorentz-corrected 1D-SAXS intensity profiles. (b) Change in long period L during the degradation.*

The $T_{m1}$ and $T_{m2}$ are still moving towards the lower temperatures, so we can assume a moderate decrease in both lamellar thicknesses. The results from SAXS (see Figure 16 and Table 3) confirmed a decrease in long-period L that comprises the lamellae's thickness plus the amorphous layer's thickness. The data from SAXS indicate a decrease in lamellar thickness during the degradation [53].

**Table 3.** SAXS results: peak position $q_{max}$ $(nm^{-1})$ and long period $L$ $(nm)$ as a function of degradation time at 270°C.

| Time (h) | $q_{max}$ $(nm^{-1})$ | $L$ $(nm)$ |
|---|---|---|
| 0.83 | 0.5179 | 12.13 |
| 23.33 | 0.5605 | 11.21 |
| 30.00 | 0.5761 | 10.91 |

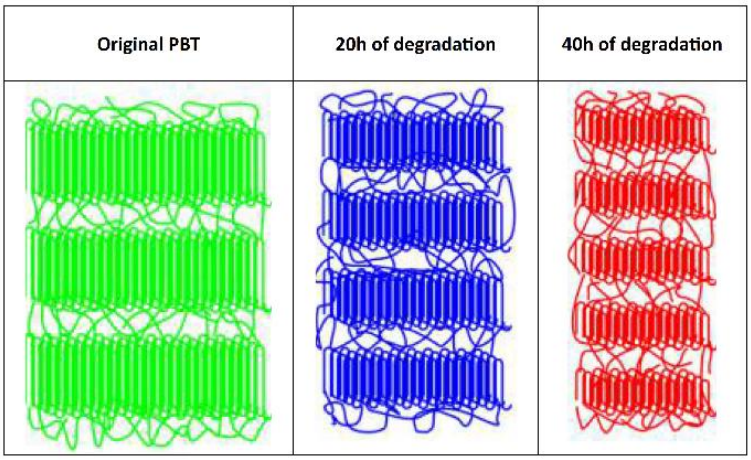


***Figure 17. Decrease in lamellar thickness during the degradation (from SAXS).***

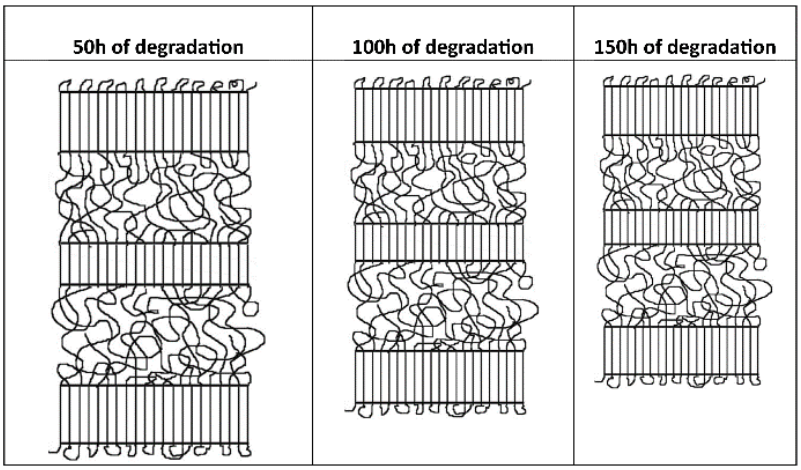


***Figure 18. Two lamellar thicknesses are possibly decreasing during the degradation (from DSC).***

## 2.2. **Mechanical and Electrical Properties Results**

Stress–strain curves are illustrated in Figure 19. Stress increases with a higher filler content for the same strain, implying a higher modulus. The reinforcing effect of the C.F. filler in the EOC matrix causes this. Even though the stress and tensile modulus are higher, EOC/CF composites remained elastic.

Several theoretical models have been described in the literature to elucidate the mechanical properties of composites containing different types of fillers. Among these models, the hydrodynamic theory proposed by Einstein [15] is considered the earliest one for spherical filler particles, which explains the viscosity of colloidal suspensions [54].

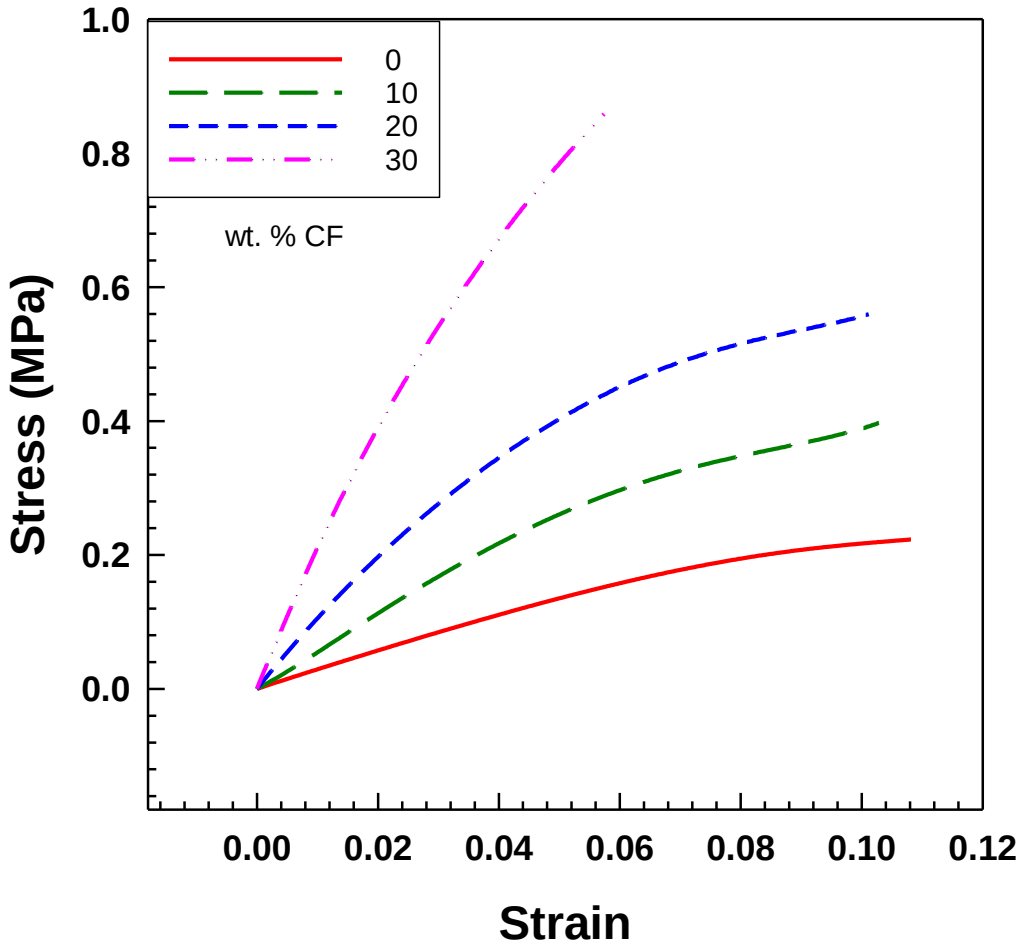


*Figure 19. Tensile stress–strain curves of EOC/CF composites measured by DMA at room temperature.*

According to Figure 20, the six-parameter model fitted the experimental data better than the four-parameter model. The parameter values of both models are included in Tables 4 and 5.

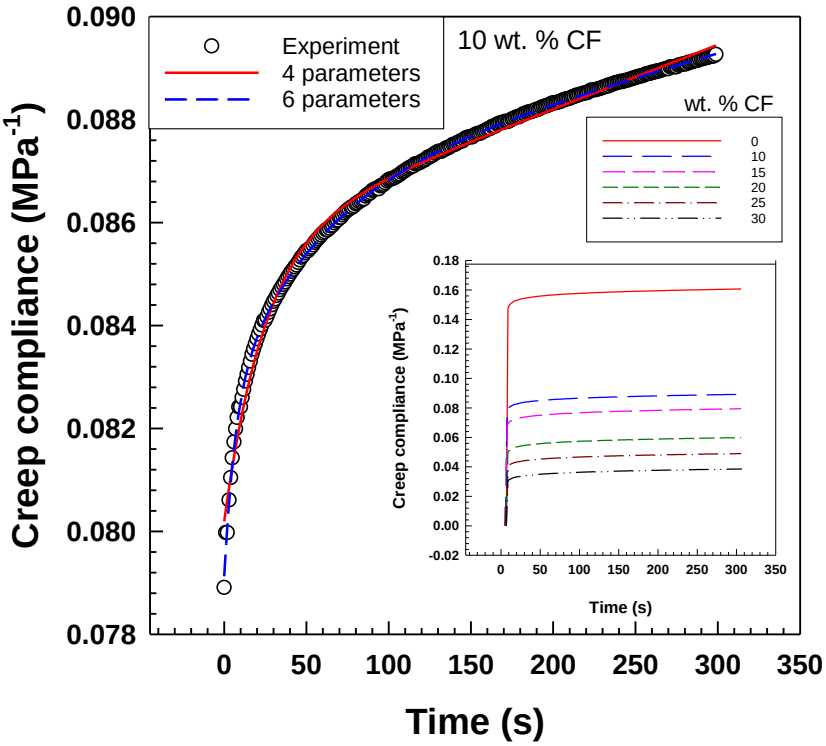


*Figure 20. Creep compliance curves measured by DMA at room temperature. Experimental data vs. Burgers model and six-parameter model.*

Table 4. Values of the four-parameter model.

| Sample | Four-Parameter Model | | | | |
|---|---|---|---|---|---|
| | $E_m$ (MPa) | $E_k$ (MPa) | $\eta_m$ (MPa·s) | $\eta_k$ (MPa·s) | $R^2$ |
| EOC | 6.7 | 142.6 | 67,114.7 | 3099.2 | 0.991 |
| EOC/10 wt% CF | 12.5 | 181.6 | 79,980.1 | 4501.2 | 0.993 |
| EOC/15 wt% CF | 14.3 | 175.1 | 76,050.2 | 4321.9 | 0.993 |
| EOC/20 wt% CF | 19.5 | 193.3 | 83,418.2 | 5017.1 | 0.992 |
| EOC/25 wt% CF | 24.1 | 222.2 | 92,440.7 | 6160.3 | 0.994 |
| EOC/30 wt% CF | 31.7 | 240.1 | 97,204.5 | 6803.7 | 0.994 |

Table 5. Values of the six-parameter model.

| Sample | Six-Parameter Model | | | | | | |
|---|---|---|---|---|---|---|---|
| | $E_0$ (MPa) | $\eta_0$ (MPa·s) | $E_1$ (MPa) | $\eta_1$ (MPa.s) | $E_2$ (MPa) | $\eta_2$ (MPa·s) | $R^2$ |
| EOC | 6.8 | 86,936.1 | 220.2 | 978.6 | 194.9 | 8612.1 | 0.9995 |
| EOC/10 wt% CF | 12.6 | 109,715.6 | 298.2 | 1964.3 | 244.6 | 13,323.8 | 0.9996 |
| EOC/15 wt% CF | 14.5 | 102,613.3 | 286.7 | 1684.1 | 231.4 | 12,130.8 | 0.9995 |
| EOC/20 wt% CF | 20.1 | 108,270.9 | 327.2 | 1480.5 | 239.9 | 11,713.2 | 0.9996 |
| EOC/25 wt% CF | 24.7 | 120,924.9 | 403.9 | 2206.1 | 271.9 | 14,217.2 | 0.9997 |
| EOC/30 wt% CF | 32.8 | 123,687.4 | 437.8 | 2034.5 | 286.3 | 14,497.8 | 0.9996 |

Previous research by Theravalappil et al. has shown that elastic electrically conductive composites reinforced with carbon fibres (EOC/CF) have a percolation threshold at 10 wt.% C.F. This result is lower than that observed for multi-walled carbon nanotube (MWCNT) composites due to the longer length of the carbon fibers, which allows for the formation of a conductive path at a lower concentration [55]. Generally, composites with filler concentrations close to the percolation threshold exhibit a high electrical resistance and gauge factor [56], making it difficult to measure their electrical properties accurately.

The strain dependence of resistance change for elastic electrically conductive (EOC) composites with varying weight percentages of C.F. (15, 20, and 25 wt.%) is depicted in Figure 21 and Table 6. The graph depicts the relationship between the strain, tensile stress, and calibrated weights ranging from 20 to 500 g. Unexpectedly, the resistance change decreases to negative values. This observation is significant as it suggests that the composite material exhibits non-linear behaviour under stress, and its electrical properties may not be suitable for specific sensor applications.

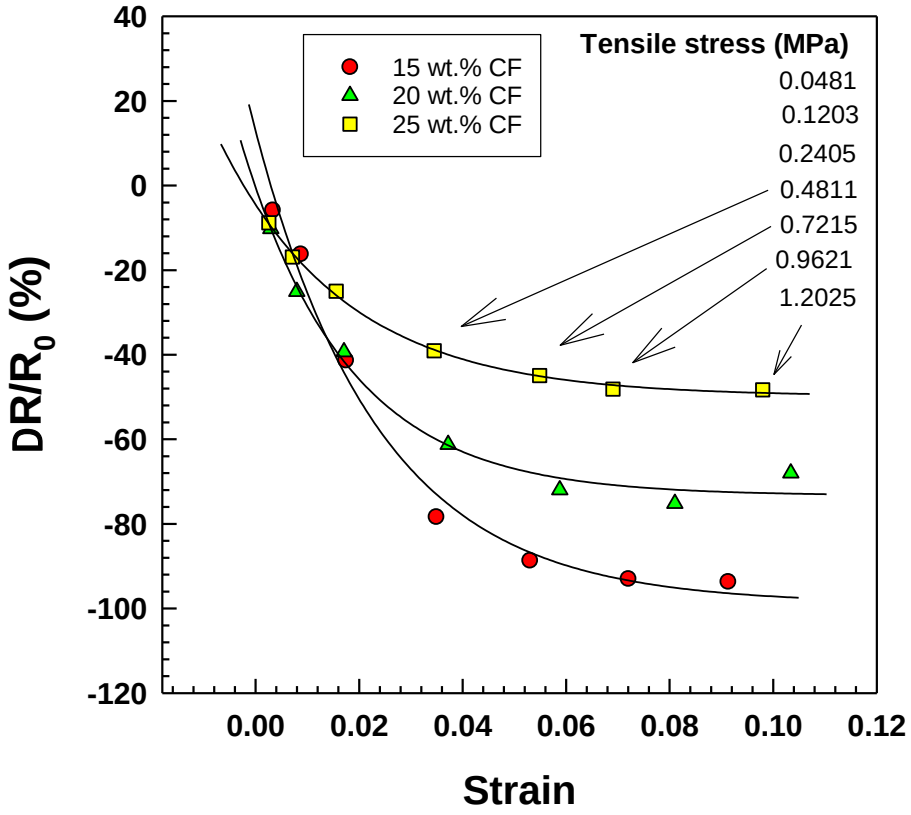


*Figure 21. Strain dependence of resistance change for EOC/CF composites with various tensile stresses.*

Table 6. Values of negative resistance change.

| wt.% C.F. | $y_0$ | a | b | $R^2$ |
|---|---|---|---|---|
| 15 | −98.82 | 111.8 | 41.96 | 0.9886 |
| 20 | −73.32 | 72.92 | 48.76 | 0.9876 |
| 25 | −49.85 | 45.36 | 41.06 | 0.9978 |

As can be seen in Figure 22, resistivity variations were observed during multiple loading and unloading cycles at a tensile stress of 1.202 MPa. The results indicate that the loading/unloading process is consistent across two cycles and a prolonged period, with no substantial changes in resistivity. Furthermore, the resistivity levels oscillate between two values, indicating the stability of the material. These findings highlight the importance of repeatability in pressure and strain sensors, as it ensures consistency in measurement accuracy over time [57].

Therefore, the ability of a material to maintain stable resistivity values during loading/unloading cycles is a critical factor to consider when selecting materials for use in pressure and strain sensors. The findings of this study suggest that carbon fibre-based composites may be suitable for use in these applications due to their ability to maintain stable resistivity values over prolonged periods.

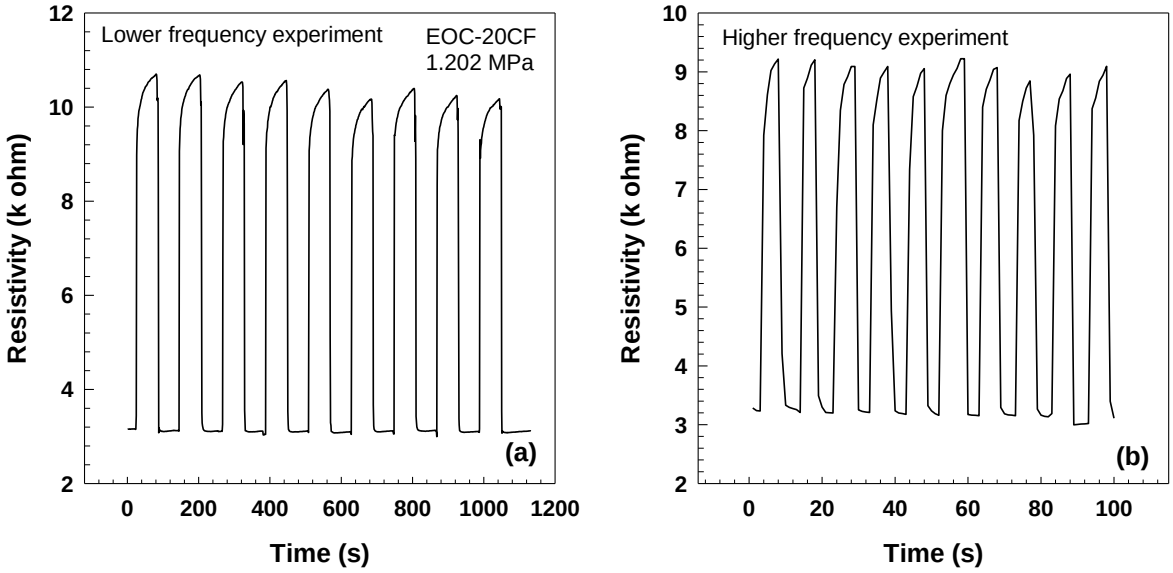


*Figure 22. Resistivity vs. time for loading/unloading cycles after (a) 1 min and (b) 5 s of EOC composite with 20 wt.% CF and tensile stress 1.202 MPa.*

# CONCLUSION

In summary, this doctoral thesis has thoroughly investigated the complex interplay between crystallization dynamics, electroconductivity, and mechanical properties in selected engineering polymers and their blends. The overarching objective was to elucidate the intricate relationships governing these fundamental properties and their implications for advanced material applications. The research commenced with a meticulous examination of the influence of thermal degradation on the crystallization of Poly(butylene terephthalate) (PBT). This investigation revealed a significant shift in crystallization temperature, signifying profound modifications. This shift occurred in distinct phases, involving an initial rise, a steep decrease, and subsequent degradation-induced changes. The study also observed corresponding trends in crystallinity and crystallization kinetics, focusing on the influence of differing lamellar thicknesses. These findings underscore the intricate nature of PBT's crystallization behaviour under thermal degradation, contributing to a broader understanding of polymer degradation and its implications for crystallization processes. Furthermore, the research delved into the intricate terrain of Poly(butylene terephthalate) crystallization kinetics, particularly in response to various fusion temperatures. Empirical results revealed a crucial correlation between fusion temperature and the resultant heat flow curve, unveiling a nuanced interplay between crystallinity and heat flow profile. The Ozawa and Avrami models were adeptly employed to elucidate crystallization kinetics, affirming the role of fusion temperature in nucleation and crystal growth mechanisms. These findings hold promise for optimizing processing parameters and enhancing material attributes across diverse applications. Moreover, the study explored the intricate interplay between fusion temperature, duration, and nonisothermal crystallization kinetics in polyamide 6 (PA6). The research unveiled insights into nucleation centers, crystallization temperature shifts, and kinetics using advanced analytical techniques. The models illuminate the complex relationship between fusion temperature and crystallization processes, furthering our comprehension of polymer material processing. Lastly, the research investigated the integration of carbon fibres within an elastic polymer matrix, yielding EOC/CF composites. The study meticulously analyzed the resulting mechanical attributes and morphology alongside implications for electroconductivity. The investigation demonstrated a marked enhancement in tensile modulus and stress through various analytical methodologies while maintaining elasticity. Moreover, it delved into electrical properties, revealing a critical percolation threshold in the composites. These results suggest the potential for advanced composites, particularly for applications in electronics engineering. In conclusion, this doctoral thesis has comprehensively explored the intricate relationships among crystallization, electroconductivity, and mechanical properties within engineering polymers and blends. The findings of this research

have far-reaching implications for material design and applications, paving the way for innovative advancements in diverse fields.

# REFERENCES


[1] Valerga AP, Fernandez-Vidal SR, Girot F, Gamez AJ. On the Relationship between Mechanical Properties and Crystallisation of Chemically Post-Processed Additive Manufactured Polylactic Acid Pieces. Polymers (Basel). 2020;12(4). https://doi.org/10.3390/polym12040941.

[2] Ma X-l, Wen L-h, Wang S-y, Xiao J-y, Li W-h, Hou X. Inherent relationship between process parameters, crystallization and mechanical properties of continuous carbon fiber reinforced PEEK composites. Defence Technology. 2023;24:269-284. https://doi.org/https://doi.org/10.1016/j.dt.2022.04.010.

[3] Kim N, Lienemann S, Petsagkourakis I, Alemu Mengistie D, Kee S, Ederth T, Gueskine V, Leclère P, Lazzaroni R, Crispin X, Tybrandt K. Elastic conducting polymer composites in thermoelectric modules. Nature Communications. 2020;11(1):1424. https://doi.org/10.1038/s41467-020-15135-w.

[4] McKeen L. 3 - Introduction to the Physical, Mechanical, and Thermal Properties of Plastics and Elastomers. In: McKeen L, editor. The Effect of Sterilization on Plastics and Elastomers (Third Edition). Boston: William Andrew Publishing; 2012. p. 57-84.

[5] Cheng SZD, Jin S. Chapter 5 - Crystallization and melting of metastable crystalline polymers. In: Cheng SZD, editor. Handbook of Thermal Analysis and Calorimetry: Elsevier Science B.V.; 2002. p. 167-195.

[6] Groeninckx G, Vanneste M, Everaert V. Crystallization, Morphological Structure, and Melting of Polymer Blends. In: Utracki LA, editor. Polymer Blends Handbook. Dordrecht: Springer Netherlands; 2003. p. 203-294.

[7] Zhao D, Yan D, Fu X, Zhang N, Yang G. Rheological and Crystallization Properties of ABS/PA6-Compatibilized Blends via In Situ Reactive Extrusion. Acs Omega. 2020;5(25):15257-15267. https://doi.org/10.1021/acsomega.0c01298.

[8] Sumita M, Sakata K, Asai S, Miyasaka K, Nakagawa H. Dispersion of fillers and the electrical conductivity of polymer blends filled with carbon black. Polymer Bulletin. 1991;25(2):265-271. https://doi.org/10.1007/BF00310802.

[9] Rahaman M, Aldalbahi A, Govindasami P, Khanam NP, Bhandari S, Feng P, Altalhi T. A New Insight in Determining the Percolation Threshold of Electrical Conductivity for Extrinsically Conducting Polymer Composites through Different Sigmoidal Models. Polymers2017.

[10] Lemanowicz M, Mielańczyk A, Walica T, Kotek M, Gierczycki A. Application of Polymers as a Tool in Crystallization -A Review. Polymers. 2021;13:2695. https://doi.org/10.3390/polym13162695.

[11] Papageorgiou G, Achilias D, Bikiaris D, Karayannidis G. Isothermal and nonisothermal crystallization kinetics of branched and partially crosslinked PET : DSC study. Journal of Thermal Analysis and Calorimetry. 2006;84:85-89. https://doi.org/10.1007/s10973-005-7366-4.

[12] Avrami M. Kinetics of Phase Change. I General Theory. The Journal of Chemical Physics. 1939;7:1103. https://doi.org/10.1063/1.1750380.

[13] Huang JW, Wen YL, Kang CC, Yeh MY, Wen SB. Morphology, melting behavior, and nonisothermal crystallization of poly(butylene terephthalate)/poly(ethylene-co-methacrylic acid) blends. Thermochimica Acta. 2007;465(1-2):48-58. https://doi.org/10.1016/j.tca.2007.09.004.

[14] Papageorgiou GZ, Achilias DS, Bikiaris DN. Crystallization Kinetics of Biodegradable Poly(butylene succinate) under Isothermal and Nonisothermal Conditions. 2007;208(12):1250-1264. https://doi.org/https://doi.org/10.1002/macp.200700084.

[15] Svoboda P. Influence of Branching Density in Ethylene-Octene Copolymers on Electron Beam Crosslinkability. Polymers2015. p. 2522-2534.

[16] Zykova A, Pantyukhov P, Popov A. Mechanical properties of ethylene-octene copolymer (EOC) - lignocellulosic fillers biocomposites in dependence to filler content. AIP Conference Proceedings. 2016;1736(1):020123. https://doi.org/10.1063/1.4949698.

[17] Rajeshbabu R, Gohs U, Naskar K, Thakur V, Wagenknecht U, Heinrich G. Preparation of polypropylene (P.P.)/ethylene octene copolymer (EOC) thermoplastic vulcanizates (TPVs) by high energy electron reactive processing. Radiation Physics and Chemistry. 2011;80(12):1398-1405. https://doi.org/https://doi.org/10.1016/j.radphyschem.2011.07.001.

[18] Tesarikova A, Merinska D, Kalous J, Svoboda P. Ethylene-Octene Copolymers/Organoclay Nanocomposites: Preparation and Properties. Journal of Nanomaterials. 2016;2016:1-13. https://doi.org/10.1155/2016/6014064.

[19] Kong Y, Hay JN. The measurement of the crystallinity of polymers by DSC. Polymer. 2002;43(14):3873-3878. https://doi.org/https://doi.org/10.1016/S0032-3861(02)00235-5.

[20] Drzeżdżon J, Jacewicz D, Sielicka A, Chmurzyński L. Characterization of polymers based on differential scanning calorimetry based techniques. TrAC Trends in Analytical Chemistry. 2019;110:51-56. https://doi.org/https://doi.org/10.1016/j.trac.2018.10.037.
[21] Al-Qatami O, Mazzanti G. The effect of the sample pan position on the determination of the specific heat capacity for lipid materials using heat flux DSC. Thermochimica Acta. 2022;710:179148. https://doi.org/https://doi.org/10.1016/j.tca.2022.179148.
[22] Chen Z, Ding Y, Pacheco-torgal F, Zhang Y. 4 - Self-sensing concrete with nanomaterials. In: Pacheco-Torgal F, Diamanti MV, Nazari A, Granqvist CG, editors. Nanotechnology in Eco-Efficient Construction: Woodhead Publishing; 2013. p. 53-74.
[23] Mironov VS, Kim JK, Park M, Lim S, Cho WK. Comparison of electrical conductivity data obtained by four-electrode and four-point probe methods for graphite-based polymer composites. Polymer Testing. 2007;26:547-555. https://doi.org/10.1016/j.polymertesting.2007.02.003.
[24] Topcu A, Daricik F, Aydin K, Celik S. Electrical Properties of the Carbon Nano tube (CNT) Reinforced Composite Plates for the PEM Fuel Cell Bipolar Plate Application2021.
[25] Nasr A, Mrhálek O, Svoboda P. Elastic Electrically Conductive Composites Based on Vapor-Grown Carbon Fibers for Use in Sensors. Polymers2023.
[26] Chen D, Li J, Yuan Y, Gao C, Cui Y, Li S, Liu X, Wang H, Peng C, Wu Z. A Review of the Polymer for Cryogenic Application: Methods, Mechanisms and Perspectives. Polymers (Basel). 2021;13(3). https://doi.org/10.3390/polym13030320.
[27] An Q, Hong C, Wen H. Fracture Patterns of Rocks Observed under Cryogenic Conditions Using Cryo-Scanning Electron Microscopy. Processes2023.
[28] Oliver RC, Rolband LA, Hutchinson-Lundy AM, Afonin KA, Krueger JK. Small-Angle Scattering as a Structural Probe for Nucleic Acid Nanoparticles (NANPs) in a Dynamic Solution Environment. Nanomaterials (Basel). 2019;9(5). https://doi.org/10.3390/nano9050681.
[29] Bogan M, Boutet S, Barty A, Benner H, Frank M, Lomb L, Shoeman R, Starodub D, Seibert M, Hau-Riege S, Woods B, DeCorwin-Martin P, Bajt S, Schulz J, Rohner U, Iwan B, Timneanu N, Marchesini S, Schlichting I, Chapman H. Single-shot femtosecond x-ray diffraction from randomly oriented ellipsoidal nanoparticles. PHYSICAL REVIEW SPECIAL TOPICS-ACCELERATORS AND BEAMS. 2010;13. https://doi.org/10.1103/PhysRevSTAB.13.094701.
[30] Lewandowski A, Wilczyński K. Modeling of Twin Screw Extrusion of Polymeric Materials. Polymers2022.
[31] Uitterhaegen E, Evon P. Twin-screw extrusion technology for vegetable oil extraction: A review. Journal of Food Engineering. 2017;212:190-200. https://doi.org/https://doi.org/10.1016/j.jfoodeng.2017.06.006.
[32] Mikulionok IO. Screw extruder mixing and dispersing units. Chemical and Petroleum Engineering. 2013;49(1):103-109. https://doi.org/10.1007/s10556-013-9711-y.
[33] Colas D, Doumeng C, Pontalier PY, Rigal L. Twin-screw extrusion technology, an original solution for the extraction of proteins from alfalfa (Medicago sativa). Food and Bioproducts Processing. 2013;91(2):175-182. https://doi.org/https://doi.org/10.1016/j.fbp.2013.01.002.
[34] Huerta E, Corona Hdez J, Oliva A, Aviles F, González-Hernández J. Universal testing machine for mechanical properties of thin materials. Revista mexicana de física. 2010;56:317-322.
[35] Johns J, Rao V. Mechanical properties of M.A. compatibilized NR/CS blends. Fibers and Polymers. 2009;10(6):761-767. https://doi.org/10.1007/s12221-009-0761-x.
[36] Bartczak Z, Galeski A. Mechanical Properties of Polymer Blends. In: Utracki LA, Wilkie CA, editors. Polymer Blends Handbook. Dordrecht: Springer Netherlands; 2014. p. 1203-1297.
[37] Cebe P, Thomas D, Merfeld J, Partlow BP, Kaplan DL, Alamo RG, Wurm A, Zhuravlev E, Schick C. Heat of fusion of polymer crystals by fast scanning calorimetry. Polymer. 2017;126:240-247. https://doi.org/10.1016/j.polymer.2017.08.042.
[38] Freire L, Combeaud C, Monge G, Billon N, Haudin JM. Transcrystallinity versus spherulitic crystallization in polyamide 66: An experimental study. Polymer Crystallization. 2019;2(1). https://doi.org/10.1002/pcr2.10028.
[39] Bassett D. Polymer Spherulites: A Modern Assessment. Journal of Macromolecular Science® Part B—Physics. 2007;B42(2):227-256. https://doi.org/10.1081/MB-120017116.
[40] Seguela R. Overview and critical survey of polyamide6 structural habits: Misconceptions and controversies. Journal of Polymer Science. 2020;58(21):2971-3003. https://doi.org/10.1002/pol.20200454.
[41] Mondal A, Sohel MA, Arif PM, Thomas S, SenGupta A. Effect of ABS on nonisothermal crystallization kinetics of polyamide 6. Journal of Thermal Analysis and Calorimetry. 2021;146(6):2489-2501. https://doi.org/10.1007/s10973-020-10443-1.
[42] Wang BB, Wang W, Wang HP, Hu GS. Isothermal crystallization kinetics and melting behavior of in situ compatibilized polyamide 6/Polyethylene-octene blends. Journal of Polymer Research. 2010;17(3):429-437. https://doi.org/10.1007/s10965-009-9329-0.
[43] Kratochvil J, Kelnar I. A simple method of evaluating nonisothermal crystallization kinetics in multicomponent polymer systems. Polymer Testing. 2015;47:79-86. https://doi.org/10.1016/j.polymertesting.2015.07.010.

[44] Alfonso GC, Ziabicki A. Memory Effects in Isothermal Crystallization .2. Isotactic Polypropylene. Colloid and Polymer Science. 1995;273(4):317-323. https://doi.org/10.1007/Bf00652344.
[45] Supaphol P, Lin JS. Crystalline memory effect in isothermal crystallization of syndiotactic polypropylenes: effect of fusion temperature on crystallization and melting behavior. Polymer. 2001;42(23):9617-9626. https://doi.org/10.1016/S0032-3861(01)00507-9.
[46] Uthaipan N, Jarnthong M, Peng Z, Junhasavasdikul B, Nakason C, Thitithammawong A. Effects of cooling rates on crystallization behavior and melting characteristics of isotactic polypropylene as neat and in the TPVs EPDM/PP and EOC/PP. Polymer Testing. 2015;44:101-111. https://doi.org/10.1016/j.polymertesting.2015.04.002.
[47] Toda A, Furushima Y, Schick C. Vitrification of the Entire Amorphous Phase during Crystallization of Poly(butylene terephthalate) near the Glass-Transition Temperature. Macromolecules. 2023;56(8):3110-3118. https://doi.org/10.1021/acs.macromol.3c00137.
[48] Svoboda P, Dvorackova M, Svobodova D. Influence of biodegradation on crystallization of poly (butylene adipate-co-terephthalate). Polymers for Advanced Technologies. 2019;30(3):552-562. https://doi.org/10.1002/pat.4491.
[49] Rabello MS, White JR. Crystallization and melting behaviour of photodegraded polypropylene .2. Re-crystallization of degraded molecules. Polymer. 1997;38(26):6389-6399. https://doi.org/10.1016/S0032-3861(97)00214-0.
[50] Rodriguez EJ, Marcos B, Huneault MA. Hydrolysis of polylactide in aqueous media. Journal of Applied Polymer Science. 2016;133(44). https://doi.org/10.1002/app.44152.
[51] Saha SK, Tsuji H. Effects of rapid crystallization on hydrolytic degradation and mechanical properties of poly(L-lactide-co-epsilon-caprolactone). Reactive & Functional Polymers. 2006;66(11):1362-1372. https://doi.org/10.1016/j.reactfunctpolym.2006.03.020.
[52] Tsuji H, Shimizu K, Sato Y. Hydrolytic degradation of poly(L-lactic acid): Combined effects of U.V. treatment and crystallization. Journal of Applied Polymer Science. 2012;125(3):2394-2406. https://doi.org/10.1002/app.36498.
[53] Mani MR, Chellaswamy R, Marathe YN, Pillai VK. New Understanding on Regulating the Crystallization and Morphology of the beta-Polymorph of Isotactic Polypropylene Based on Carboxylate-Alumoxane Nucleating Agents. Macromolecules. 2016;49(6):2197-2205. https://doi.org/10.1021/acs.macromol.5b02466.
[54] Jha V, Hon AA, Thomas AG, Busfield JJC. Modeling of the effect of rigid fillers on the stiffness of rubbers. Journal of Applied Polymer Science. 2008;107(4):2572-2577. https://doi.org/10.1002/app.27324.
[55] Theravalappil R, Svoboda P, Vilcakova J, Poongavalappil S, Slobodian P, Svobodova D. A comparative study on the electrical, thermal and mechanical properties of ethylene–octene copolymer based composites with carbon fillers. Materials & Design. 2014;60:458-467. https://doi.org/10.1016/j.matdes.2014.04.029.
[56] Yan Y, Sencadas V, Zhang JS, Zu GQ, Wei DB, Jiang ZY. Processing, characterization and electromechanical behaviour of elastomeric multiwall carbon nanotubes-poly (glycerol sebacate) nanocomposites for piezoresistive sensors applications. Composites Science and Technology. 2017;142:163-170. https://doi.org/10.1016/j.compscitech.2017.02.007.
[57] Slobodian P, Olejnik R, Matyas J, Babar DG. Improving sensitivity of the polyurethane/CNT laminate strain sensor by controlled mechanical preload. IOP Conference Series: Materials Science and Engineering. 2016;108(1):012022. https://doi.org/10.1088/1757-899X/108/1/012022.

# Study the Crystallization, Electroconductivity and Mechanical Properties in Selected Engineering Polymers and Blends

Studium krystalizace, elektrické vodivosti a mechanických vlastností vybraných inženýrských polymerů a směsí

Doctoral Thesis Summary

Published by: Tomas Bata University in Zlín,

nám. T. G. Masaryka 5555, 760 01 Zlín.

Edition: published electronically

Typesetting by: Ahmed Nasr



Publication year: 2023

First Edition

ISBN 978-80-7678-216-7